SUPPORTING INFORMATION

Channels modestly impact compartment-specific ATP levels during *Bacillus subtilis* sporulation and a rise in the mother cell ATP level is not necessary for Pro-σ^K cleavage

Daniel Parrell, Lee Kroos*

Department of Biochemistry and Molecular Biology, Michigan State University, East Lansing, Michigan, USA

For correspondence. *E-mail kroos@msu.edu; Tel. (+1) 517 355 9726; Fax (+1) 517 353 9334.

Results

Luciferin rapidly enters cells and is not significantly depleted during sporulation

We performed two experiments to determine the effects of adding luciferin at different times PS. In these experiments, starvation was initiated in flasks; at 2 h PS, culture aliquots were transferred to a 96-well plate, and luciferin was added at different times PS. In the first experiment, luciferin addition at 2 h was compared with addition at 2.5 h. After 1 min of vigorous shaking, luminescence intensity was measured, then shaking continued until the next measurement. Luminescence was observed after luciferin addition at 2 h, increased by 2.5 h, decreased by 3.5 h, then remained about the same until 6 h, for both promoter fusions to *luc H245F* (Fig. S3A). Very similar results were observed when luciferin was added at 2.5 h rather than at 2 h, suggesting that luciferin rapidly enters both the MC and the FS at 2.5 h. Previously, it was shown that luciferin enters growing *B. subtilis* within 1 min (Mirouze *et al.*, 2011). In our second experiment, luciferin addition at 2.5 h was compared with addition at 3 to 6 h. For both promoter fusions to *luc H245F*, luminescence intensity was similar or greater when luciferin was added at 2.5 h than when it was added later (Fig. S3B and S3C), indicating that luciferin was not significantly depleted by Luc H245F activity between 2.5 and 6 h. Based on the results of these experiments, to measure luminescence intensity during sporulation, starvation was initiated in flasks and at 2 h PS culture aliquots were transferred to a 96-well plate in which luciferin had been added to the wells.

The Luc H245F level can be used to normalize luminescence intensity measurements

To account for different levels of Luc H245F at different times PS, we performed control experiments to test whether the Luc H245F level measured by immunoblot could be used for normalization of luminescence intensity measurements. We reasoned that growing *B. subtilis* would have a particular cellular ATP concentration, which should yield a very similar ratio of luminescence intensity to Luc H245F protein level, over a range in which the Luc H245F level was limiting for luminescence. To

produce Luc H245F at different levels, the IPTG-inducible *hyperspank* promoter was fused to *luc H245F* and a strain bearing the fusion at the *amyE* locus was created. Aliquots of the growing strain were placed into a 96-well plate containing luciferin in each well and a range of IPTG concentrations in different wells. After 15 and 30 min of continued growth with vigorous shaking, the luminescence intensity and absorbance at 595 nm of each well was measured, and after the 30-min measurements, each aliquot was collected for determination of the Luc H245F protein level by immunoblot. The range of IPTG concentrations used (0 to 100 μM) was designed to produce luminescence and immunoblot signals after 30 min that would span the range of signals observed during sporulation, based on preliminary experiments.

As expected, the luminescence intensity increased with increasing IPTG concentration after 15 min and to a greater extent after 30 min (Fig. S4A). IPTG did not affect absorbance at 595 nm after 15 or 30 min (Fig. S4B), suggesting that neither production of Luc H245F nor its utilization of ATP became limiting for growth. Also, IPTG did not change the concentration of ATP in extracts of boiled cells after 30 min of growth (Fig. S4C). As expected, the Luc H245F protein level increased with increasing IPTG concentration (Fig. S4D and S4E). Importantly, the normalized luminescence intensity (i.e., luminescence intensity/Luc H245F protein level) was very similar (0.0077 ± 0.0005) over the range of 10 to 100 μM IPTG (Fig. S4F). We note the large error bars at 0 and 10 μM IPTG due to low luminescence (Fig. S4A) and Luc H245F immunoblot signals (Fig. S4D and S4E). Nevertheless, the very similar normalized luminescence intensity (Fig. S4F) shows that Luc H245F is limiting for luminescence over a broad range (Fig. S4A, S4D, and S4E) in growing cells. Our preliminary experiments suggested that Luc H245F would be limiting for luminescence over a broad range in sporulating cells as well, because the normalized luminescence intensity values during sporulation exceeded the value of 0.0077 during growth. Hence, the pool of ATP available to Luc H245F produced in the MC or the FS appeared to exceed the pool of ATP available to Luc H245F produced in growing cells (see Discussion below), and in

both cases the available ATP concentration was sufficient to saturate the enzyme produced over a broad range of levels. Therefore, we measured both luminescence intensity and the Luc H245F protein level in our experiments, and we report the normalized luminescence intensity as the "relative ATP concentration."

Efforts to build a FRET-based ATP sensor

Our initial effort to measure cellular ATP concentrations aimed to use a Fluorescence Resonance Energy Transfer (FRET) biosensor. In recent years, fluorescence-based biomolecule sensors have provided many useful tools for researchers. These sensors have often relied on FRET between pairs of fluorescent proteins linked to a "sensor" protein which brings the FRET pair together or apart in response to a particular biomolecule. One such sensor is the ATP sensor AT1.03 (Imamura *et al.*, 2009). This sensor uses a blue (mseCFP) and yellow (cp173-mVenus) pair of fluorescent proteins fused to the ATP-binding domain of the epsilon subunit of *B. subtilis* ATP synthase. When ATP is bound, the FRET pair is brought close enough that FRET can occur. By using AT1.03 and a confocal microscope, we hoped to achieve measurements of cellular ATP levels at single-cell resolution. An additional benefit to using AT1.03 was that variants developed by Imamura *et al.* (Imamura *et al.*, 2009) work at different ranges of ATP concentrations, allowing the sensor to be tuned to specific applications. AT1.03 was successfully used to measure ATP levels in human cell lines (Imamura *et al.*, 2009, Ando *et al.*, 2012); however, no studies to our knowledge have successfully used AT1.03 in bacteria.

DNA constructs were built in which the gene for AT1.03 was fused to the mother cell-specific *spoIID* promoter or to the forespore-specific *spoIIQ* promoter (Sharp & Pogliano, 2002) in plasmids that allow for gene replacement by homologous recombination at the chromosomal *amyE* locus of *B. subtilis* (Shimotsu & Henner, 1986). Additionally, the gene for AT1.03 was codon optimized (designated $AT1.03_{opt}$) for expression in *B. subtilis* (sequence available on request) and fused to the *spoIIQ* promoter

or the IPTG-inducible *spank* promoter in plasmids that allow gene replacement at *amyE*, or fused to the IPTG-inducible *spac* promoter in an autonomously replicating multicopy plasmid (see Table S2 for plasmid construction details and resulting bacterial strains).

B. subtilis strains with a compartment-specific promoter fused to the genes for AT1.03 or $AT1.03_{opt}$ were starved to induce sporulation. Strains with an IPTG-inducible promoter fused to the gene encoding $AT1.03_{opt}$ were grown in LB medium at 37°C with shaking until reaching an optical density at 600 nm of 0.5-0.6, then IPTG (0.5 mM) was added and incubation continued for 2 h. For comparison, *B. subtilis* strains with a multicopy plasmid in which the genes for CFP_{opt} or YFP_{opt} (codon optimized for expression in *Bacillus anthracis*) were fused to the constitutive *B. anthracis pagA* promoter (Table S2), were grown in LB medium at 37°C with shaking until reaching an optical density at 600 nm of 0.5-0.6. These strains synthesize fluorescent proteins abundantly and fluoresce brightly. Samples for microscopy were collected and flash frozen in liquid nitrogen. These samples were later thawed and observed using an Olympus FluoView FV1000 confocal laser scanning microscope. Blue fluorescent proteins were excited using a 458 nm argon laser. Emission was split to one channel using a DM458/515 dichroic mirror and was detected in that channel using a 480-495 nm band pass filter. Yellow fluorescent proteins were excited using a 514 nm argon laser. Emission was split to a second channel using a DM458/515 dichroic mirror and was detected in the second channel using a BA535-565 nm band pass filter. Samples to compare accumulation of fluorescent proteins were prepared from equivalent amounts of cells based on the optical density at 600 nm of the cultures (Zhou & Kroos, 2004) and immunoblot analysis was performed using anti-GFP antibodies.

All of the strains designed to synthesize AT1.03 or $AT1.03_{opt}$ showed little or no fluorescence above background. A representative cell from the strain with an IPTG-inducible gene encoding $AT1.03_{opt}$ on a multicopy plasmid demonstrates the low signal-to-noise ratio under conditions that allowed us to see fluorescence from cells (Fig. S14A, top panels). Additionally, the presence of fluorescent foci and

filamentous cells upon IPTG induction suggests that the sensor protein forms inclusion bodies and may be toxic. IPTG induction from a single chromosomal copy during growth or expression from a compartment-specific promoter during sporulation yielded similar low levels of fluorescence and also displayed foci indicative of inclusion bodies (data not shown). In contrast, the strains constitutively expressing genes for CFP_{opt} or YFP_{opt} exhibited relatively intense fluorescence, as expected (Fig. S14A, bottom panels). Immunoblot analysis using anti-GFP antibodies confirmed poor accumulation of $AT1.03_{opt}$ in the IPTG-inducible strains (Fig. S14B). Similar accumulation was observed during sporulation of strains with compartment-specific promoters fused to genes encoding AT1.03 or $AT1.03_{opt}$ (data not shown). As expected, CFP_{opt} and YFP_{opt} accumulated abundantly in the strains designed to produce these proteins constitutively (Fig. S14B). Taken together, these results show that AT1.03 and $AT1.03_{opt}$ are poorly produced in *B. subtilis*.

Discussion

Comparisons between the relative ATP concentration determined using Luc H245F and the concentration of ATP in cell extracts

We compared two very different methods of measuring the cellular ATP concentration in three of the experiments reported herein. The results of those comparisons are summarized in Table S3. Both methods indicated a five-fold to six-fold decrease in ATP upon treatment at 3.5 h PS with the ionophore FCCP (100 μM) for 15 min (-/+ FCCP ratio in the top section of Table S3). These results, with sporulating cells, are in good agreement with a four-fold decrease in ATP upon treatment of growing cells with CCCP (100 μM) for 15 min, measured using an extraction approach (Strahl & Hamoen, 2010). Since CCCP and FCCP are proton ionophores that rapidly dissipate pmf, our results suggest that pmf continues to drive ATP synthesis by 3.5 h PS. We note that the relative ATP concentration determined using Luc H245F indicated a similar decrease in the MC and the FS (Table S3). This result could be due to the channels

connecting the two compartments during engulfment, if the channels allow rapid equilibration of ATP levels between compartments. However, FCCP treatment later during sporulation (at 4 to 6 h) also caused a decrease in ATP (fivefold to tenfold, Fig. S5). This finding requires a different explanation, since after 3.5 h, channel proteins diminish (Fig. 5, wild-type cells). The finding suggests that a pmf across the inner FS membrane drives ATP synthesis in the FS after engulfment completion and channel destruction. In any case, the similar fold decrease in ATP after FCCP treatment observed by the two methods (Table S3) supports their use in measuring cellular ATP concentrations.

The two methods also yielded similar results when testing the effect of IPTG addition to growing cells engineered to produce Luc H245F under control of an IPTG-inducible promoter. Both methods indicated little or no change in the cellular ATP concentration upon treatment with IPTG (100 μM) for 30 min (-/+ IPTG ratio in the middle section of Table S3). Induction of Luc H245F was not expected to change ATP levels significantly, considering the many ATP-dependent processes that are ongoing during growth. In meeting this expectation, use of the two methods was further supported.

The two methods yielded somewhat different results upon comparing 6 h versus 3.5 h PS. The total relative ATP concentration (i.e. the sum of the MC and the FS compartments) measured using Luc H245F indicated a 6/3.5 h ratio of 1.6, whereas the ATP concentration of cell extracts indicated a ratio of 0.6 (bottom section of Table S3). One possible explanation of the different ratios is that the pool of ATP available to Luc H245F changes differently during sporulation than the total ATP pool extractable by boiling the cells. Alternatively or in addition, the different ratios may reflect the contribution of non-sporulating cells to the ATP concentration measured by the extraction method, but not to the relative ATP concentration measured using Luc H245F.

At the bottom of each section of Table S3, we report the ratios of relative ATP concentrations measured using Luc H245F to the ATP concentrations directly measured in cell extracts. We interpret these ratios to reflect the available ATP pool as a proportion of the total ATP pool. As expected, there

was little or no change in the ratio 15 min after ATP synthesis was stopped by FCCP addition at 3.5 h PS (top section of Table S3) or 30 min after Luc H245F was induced by IPTG addition to growing cells (middle section of Table S3). Strikingly, the ratios during sporulation are about 100-fold greater than during growth. Non-sporulating cells cannot account for such a large difference in the ratios, since >60% of the cells were sporulating at 3.5 h PS (i.e. non-sporulating cells could account for a difference in the ratios of about twofold at most). Rather, the large difference in the ratios suggests that the available ATP pool is a much larger proportion of the total ATP pool during sporulation than during growth. Growing cells appear to have a large total ATP pool (6 μM in extracts), but a small available ATP pool (0.005 to 0.008 AU), whereas sporulating cells appear to be the opposite, having a relatively small total ATP pool (0.48 μM in extracts without FCCP treatment) and a relatively large available ATP pool (0.056 AU total without FCCP treatment). A plausible explanation for the apparent change in the available versus the total ATP pools is that the balance between ATP utilization and synthesis shifts during the transition from growth (high utilization and synthesis result in a low available/total ATP pool ratio) to 3.5 h PS (less utilization increases the available pool and less synthesis decreases the total pool). It would be interesting to compare the ATP pool available to Luc H245F (using IPTG-inducible expression of *luc H245F*) with the total ATP pool extracted by boiling cells at additional times during the transition from growth to sporulation, including under different conditions that induce sporulation and in mutants that affect metabolism (Fortnagel & Freese, 1968, Hutchison & Hanson, 1974, Klofat *et al.*, 1969, Freese & Fortnagel, 1969, Yousten & Hanson, 1972).

As noted previously, extraction methods are designed to release ATP from macromolecules in order to reflect the total ATP pool (Schneider & Gourse, 2004). Our results suggest that the total ATP pool decreases by 40% between 3.5 and 6 h PS (Fig. S6; summarized in the bottom section of Table S3). Previous studies of *B. subtilis* by various extraction methods suggested that the total ATP pool remains approximately constant during sporulation (Hutchison & Hanson, 1974, Klofat *et al.*, 1969), whereas the

pool appeared to be very low in dormant spores (Setlow & Kornberg, 1970). The ATP level in spores may decline for several days after release from the MC, as molecular changes occur during entry into dormancy (Segev *et al.*, 2012). In isolated forespores of *B. megaterium*, the ATP/total adenine nucleotide ratio decreased about threefold between 3 and 5.5 h PS (Singh *et al.*, 1977). Our results in *B. subtilis* suggest that the FS pool of ATP available to Luc H245F increases 1.8-fold between 4 and 6 h (Fig. 3D; note that a 1.4-fold increase between 3.5 and 6 h is reported in Table S3). It would be interesting to compare the FS pool of ATP available to Luc H245F in *B. megaterium* with that in *B. subtilis.*

Experimental procedures

ATP assay and preparation of cell extracts

Firefly lantern extract (Sigma-Aldrich catalog #FLE250) was used according to the manufacturer's instructions for bioluminescent determination of ATP concentration. Briefly, firefly lantern extract solution (100 μL) supplemented with D-luciferin (1 mM) was transferred to a 96-well plate (black walls, clear bottom), sample (20 μL) was added, the solution was mixed by pipetting 5 times, then luminescence intensity was measured 20 s later, which was the time required to obtain a reading on the Filtermax F5 plate reader. A control sample of water was measured in parallel and the resulting background luminescence was subtracted.

Samples with a known concentration of ATP were used to calibrate the ATP assay for each experiment, which began by preparing enough of the firefly lantern extract solution plus D-luciferin for all the assays to be performed. The solution was warmed for 5 min at 37°C, then centrifuged at 14,100 × *g* for 1 min, and 100 μL of the supernatant was used in each assay. For the samples of known ATP concentration, the luminescence intensity in arbitrary units was plotted versus the ATP concentration and the trend line of the data was calculated using Excel (Microsoft).

Samples (1 mL from a subculture or from 5 wells of a 96-well plate) for preparation of cell extracts were centrifuged at 14,100 × *g* for 3 min, the supernatants were removed, and the cell pellets were stored at -80°C. To prepare a cell extract, 100 μL of buffer (20 mM glycine, 50 mM $MgSO_4$, 4 mM Na_2EDTA, pH 7.4) was mixed with a cell pellet by pipetting 10 times, the mixture was heated for 45 s in a boiling water bath, then centrifuged at 14,100 × *g* for 1 min, and a sample (20 μL) of the supernatant was assayed as described above. The ATP concentration of the extract was calculated using the trend line equation from samples of known ATP concentration determined in the same experiment.

Induction of Luc H245F during growth

B. subtilis strain BDP121 bearing the $P_{hyperspank}$-*luc H245F* fusion was grown in LB medium (Sambrook *et al.*, 1989) in flasks with shaking (350 rpm) at 37°C until the culture reached the exponential phase of growth (30-40 Klett units). Culture aliquots (200 μL) were transferred to a 96-well plate containing D-luciferin and IPTG (4.5 mM and 0-100 μM final concentrations, respectively), and shaken vigorously (orbital, high setting) at 37°C using a Filtermax F5 plate reader (Molecular Devices). At intervals, shaking was paused briefly to measure luminescence intensity and absorbance at 595 nm.

Table S1 Pro-σ^K and σ^K levels after ionophore or chloramphenicol treatment[a]

Figure 9B			
Lane	Pro-σ^K	σ^K	Pro-σ^K + σ^K
1	11,325	7,872	19,197
2	16,413	25,302	41,714
3	13,735	11,800	25,535
4	11,335	9,337	20,672
5	12,375	9,994	22,368
6	13,514	10,354	23,868
7	5,115	12,673	17,788
Figure 9D			
Lane	Pro-σ^K	σ^K	Pro-σ^K + σ^K
1	6,435	4,298	10,733
2	8,215	5,580	13,794
3	12,223	10,111	22,334
4	11,969	14,050	26,019
5	7,757	4,969	12,726
6	9,643	5,893	15,536
7	11,585	7,162	18,747
8	4,392	3,721	8,114
9	3,175	3,755	6,930
10	3,350	4,224	7,574

[a]See Figure 9 for treatments. Pro-σ^K and σ^K levels are signal intensities in arbitrary units.

Table S2 Bacterial strains, plasmids, and primers

Strain	Genotype	Construction or note	Source or reference
AG185	*spoIIAC1 trpC2*	*spoIIAC1* is a loss-of-function allele of *sigF* and is designated *sigF* below and in the text	Alan Grossman
BDR347	*spoIVFBΩpdr68 [spoIVFB-gfp(mut2) (tet^r)]*		(Rudner & Losick, 2002)
BK750	*spoIVB::ermG (erm^r)*		(Cutting *et al.*, 1991)
BTD117	*ΔspoIIIAAΩpDT21 (phleo^r)*		(Doan *et al.*, 2009)
BTD125	*ΔspoIIIAHΩpDT21 (phleo^r)*		(Doan *et al.*, 2009)
BTD141	*spoIIQ::spec^r*		(Doan *et al.*, 2009)
KS440	*spoIIG41*	*spoIIG41* is a loss-of-function allele of *sigE* and is designated *sigE* below and in the text	(Sandman *et al.*, 1988)
PY79	Prototrophic wild-type strain		(Youngman *et al.*, 1984)
SC777	*spoIIIG::cm^r bofB8*	*spoIIIG::cm^r* is a loss-of-function allele of *sigG* and is designated *sigG* below and in the text	(Cutting *et al.*, 1990)
BDP1	*amyE::P$_{spoIIQ}$-AT1.03 (cm^r)*	PY79 was transformed with pEF1	This study
BDP2	*amyE::P$_{spoIID}$-AT1.03 (cm^r)*	PY79 was transformed with pEF2	This study
BDP34	*amyE::P$_{spoIIQ}$-AT1.03$_{opt}$ (cm^r)*	PY79 was transformed with pDP4	This study
BDP36	*amyE::P$_{spank}$-AT1.03 (spec^r)*	PY79 was transformed with pDP5	This study
BDP38		PY79 was transformed with pDP6	This study
BDP40		PY79 was transformed with pSW4-CFP$_{opt}$	This study
BDP41		PY79 was transformed with pSW4-YFP$_{opt}$	This study
BDP84	*amyE::P$_{spoIID}$-luc (cm^r)*	PY79 was transformed with pDP58	This study
BDP85	*amyE::P$_{spoIID}$-luc H245F (cm^r)*	PY79 was transformed with pDP77	This study
BDP86	*amyE::P$_{spoIIQ}$-luc (cm^r)*	PY79 was transformed with pDP59	This study
BDP87	*amyE::P$_{spoIIQ}$-luc H245F (cm^r)*	PY79 was transformed with pDP78	This study
BDP92	*amyE::P$_{spoIID}$-luc H245F (cm^r), ΔspoIIIAAΩpDT21 (phleo^r)*	BDP85 was transformed with BTD117 DNA	This study
BDP93	*amyE::P$_{spoIID}$-luc H245F (cm^r), ΔspoIIIAHΩpDT21 (phleo^r)*	BDP85 was transformed with BTD125 DNA	This study
BDP94	*amyE::P$_{spoIID}$-luc H245F (cm^r), spoIIQ::spec^r*	BDP85 was transformed with BTD141 DNA	This study
BDP99	*amyE::P$_{spoIIQ}$-luc H245F (cm^r), ΔspoIIIAHΩpDT21 (phleo^r)*	BDP87 was transformed with BTD125 DNA	This study
BDP100	*amyE::P$_{spoIIQ}$-luc H245F (cm^r), spoIIQ::spec^r*	BDP87 was transformed with BTD141 DNA	This study
BDP105	*amyE::P$_{spoIIQ}$-luc H245F (cm^r), ΔspoIIIAAΩpDT21 (phleo^r)*	BDP87 was transformed with BTD117 DNA	This study
BDP106	*sigG, bofB8, spoIIQ::spec^r*	SC777 was transformed with BTD141 DNA	This study
BDP107	*sigG, bofB8, ΔspoIIIAAΩpDT21 (phleo^r)*	SC777 was transformed with BTD117 DNA	This study
BDP108	*sigG, bofB8, ΔspoIIIAHΩpDT21 (phleo^r)*	SC777 was transformed with BTD125 DNA	This study
BDP109	*sigG, bofB8, spoIVFBΩpdr68 [spoIVFB-gfp(mut2) (tet^r)]*	SC777 was transformed with BDR347 DNA	This study
BDP110	*sigG, bofB8, spoIIQ::spec^r, spoIVFBΩpdr68 [spoIVFB-gfp(mut2) (tet^r)]*	BDP106 was transformed with BDR347 DNA	This study
BDP111	*sigG, bofB8, ΔspoIIIAAΩpDT21 (phleo^r), spoIVFBΩpdr68 [spoIVFB-gfp(mut2) (tet^r)]*	BDP107 was transformed with BDR347 DNA	This study
BDP112	*sigG, bofB8, ΔspoIIIAHΩpDT21 (phleo^r), spoIVFBΩpdr68 [spoIVFB-gfp(mut2) (tet^r)]*	BDP108 was transformed with BDR347 DNA	This study
BDP113	*sigE, amyE::P$_{spoIID}$-luc H245F (cm^r)*	KS440 was transformed with BDP85 DNA	This study

BDP114	*sigE, amyE::P_{spoIIQ}-luc H245F (cm^r)*	KS440 was transformed with BDP87 DNA	This study
BDP115	*sigF, trpC2, amyE::P_{spoIID}-luc H245F (cm^r)*	AG185 was transformed with BDP85 DNA	This study
BDP116	*sigF, trpC2, amyE::P_{spoIIQ}-luc H245F (cm^r)*	AG185 was transformed with BDP87 DNA	This study
BDP117	*amyE::P_{spoIID}-luc H245F (cm^r), spoIVB::ermG (erm^r),*	BDP85 was transformed with BK750 DNA	This study
BDP118	*amyE::P_{spoIIQ}-luc H245F (cm^r), spoIVB::ermG (erm^r)*	BDP87 was transformed with BK750 DNA	This study
BDP119	*amyE::P_{spoIIQ}-luc H245F (cm^r), spoIIQ::spec^r, ΔspoIIIAAΩpDT21 (phleo^r)*	BDP100 was transformed with BTD117 DNA	This study
BDP120	*amyE::P_{spoIIQ}-luc H245F (cm^r), spoIIQ::spec^r, ΔspoIIIAHΩpDT21 (phleo^r)*	BDP100 was transformed with BTD125 DNA	This study
BDP121	*amyE::$P_{hyperspank}$-luc H245F (cm^r)*	PY79 was transformed with pDP86	This study

Plasmid	Description	Construction	Source or reference
pGL2-control vector	contains the firefly luciferase gene *luc*		Promega
pMDS13	pDG1662 containing *amyE::P_{spoIIQ}-gfp* (cm^r)		(Sharp & Pogliano, 2002)
pMDS14	pDG1662 containing *amyE::P_{spoIID}-gfp (cm^r)*		(Sharp & Pogliano, 2002)
pcDNA-AT1.03	contains the FRET-based ATP sensor gene *AT1.03*		(Imamura *et al.*, 2009)
pSW4-CFP$_{opt}$	contains *P_{pagA}-ecfp$_{opt}$*		(Sastalla *et al.*, 2009)
pSW4-YFP$_{opt}$	contains *P_{pagA}-eyfp$_{opt}$*		(Sastalla *et al.*, 2009)
pDG148	vector for autonomous replication in *B. subtilis*		(Stragier *et al.*, 1988)
pDG364	vector for gene replacement at *amyE*		(Cutting & Horn, 1990)
pDR110	vector for *P_{spank}* fusion and gene replacement at *amyE*		David Rudner
pDR111	vector for *$P_{hyperspank}$* fusion and gene replacement at *amyE*		David Rudner
pEF1	pDG364 containing *amyE::P_{spoIIQ}-AT1.03 (cm^r)*	*P_{spoIIQ}* and the first 5 codons of *spoIIQ* were amplified by PCR using pMDS13 as template and primers EF01 and EF02. The fragment was digested with BglII and XhoI. AT1.03 was amplified by PCR using pcDNA-AT1.03 as template and primers DH03 and DH04. The fragment was digested with XhoI and HindIII. The fragments were included in a three-way ligation with BamHI-HindIII-digested pDG364.	This study
pEF2	pDG364 containing *amyE::P_{spoIID}-AT1.03 (cm^r)*	*P_{spoIID}* and the first 4 codons of *spoIID* were amplified by PCR using pMDS14 as template and primers DH02 and EF07. The fragment was digested with BglII and XhoI. AT1.03 was amplified by PCR using pcDNA-AT1.03 as template and primers DH03 and DH04. The fragment was digested with XhoI and HindIII. The fragments were included in a three-way ligation with BamHI-HindIII-digested pDG364.	This study
pDP3	pUCminusMCS containing the FRET-based ATP sensor gene *AT1.03$_{opt}$*	pDP3 was constructed by Blue Heron Biotech. *AT1.03$_{opt}$* is codon optimized for expression in *B. subtilis* and is preceded by SalI, ribosome binding, and XhoI sites, and followed by HindIII and SphI sites.	This study
pDP4	pDG364 containing *amyE::P_{spoIIQ}-AT1.03$_{opt}$ (cm^r)*	*P_{spoIIQ}* and the first 5 codons of *spoIIQ* were amplified by PCR using pMDS13 and primers EF01 and EF02. The fragment was digested with BglII and XhoI. pDP3 was digested with XhoI and HindIII to produce a fragment with *AT1.03$_{opt}$*. The fragments were	This study

		included in a three-way ligation with BamHI-HindIII-digested pDG364.	
pDP5	pDR110 containing *amyE::P_{spank}-AT1.03$_{opt}$ (spec^r)*	pDP3 was digested with SalI and SphI to produce a fragment with a ribosome binding site and *AT1.03$_{opt}$*. The fragment was ligated with SalI-SphI-digested pDR110.	This study
pDP6	pDG148 containing *P_{spac}-AT1.03$_{opt}$* (kan^r)	pDP3 was digested with SalI and SphI to produce a fragment with a ribosome binding site and *AT1.03$_{opt}$*. The fragment was ligated with SalI-SphI-digested pDG148.	This study
pDP58	pDG364 containing *amyE::P_{spoIID}-luc (cm^r)*	*P_{spoIID}* and the first 4 codons of *spoIID* were amplified by PCR using pMDS14 as template and primers PDP141 and PDP175. The *luc* gene was amplified by PCR using pGL2 as template and primers PDP145 and PDP146. The fragments were used in a Gibson assembly reaction (Gibson *et al.*, 2009) with HindIII-digested pDG364.	This study
pDP59	pDG364 containing *amyE::P_{spoIIQ}-luc (cm^r)*	*P_{spoIIQ}* and the first 5 codons of *spoIIQ* were amplified by PCR using pMDS13 as template and primers PDP139 and PDP174. The *luc* gene was amplified by PCR using pGL2 as template and primers PDP145 and PDP146. The fragments were used in a Gibson assembly reaction (Gibson *et al.*, 2009) with HindIII-digested pDG364.	This study
pDP77	pDG364 containing *amyE::P_{spoIID}-luc H245F (cm^r)*	pDP58 was subjected to site-directed mutagenesis using the QuikChange kit (Stratagene) and primers PDP160 and PDP161.	This study
pDP78	pDG364 containing *amyE::P_{spoIIQ}-luc H245F (cm^r)*	pDP59 was subjected to site-directed mutagenesis using the QuikChange kit (Stratagene) and primers PDP160 and PDP161.	This study
pDP86	pDR111 containing *amyE::$P_{hyperspank}$-luc H245F (cm^r)*	To produce a fragment with a ribosome binding site and *luc H245F*, PCR was performed using pDP77 as template and primers PDP156 and PDP157. The fragment was used in a Gibson assembly reaction (Gibson *et al.*, 2009) with HindIII-digested pDR111.	This study

Primer	Sequence
DH02	CTGATCACTAGTGGATCCTGCGAATTGTTTCATATTCAGCTGC
DH03	GCGACTAGTATGGTGAGCAAGGGCGAGG
DH04	CTTAAGCTTACTCGATGTTGTG
EF01	GCCTCGAGTTTTCTTCCTCTCTCATTGTTTCATC
EF02	GCCTCGAGGCGAATTGTTTCATATTCAGCTGC
EF07	GTACAGCTTCAGGGAGCTGAAG
PDP139	GACCGGCGCTCAGGGATCCTAGAAGTTCGCTAGCGCCATAAGTGAGCGGATGCCAAG
PDP141	GACCGGCGCTCAGGGATCCTAGAAGTTCGCTAGCGTTGATTTAGCAAACTATATC
PDP145	ATGGAAGACGCCAAAAACATAAAG
PDP146	AGCTGTCAAACATGAGAATTCGATATTACAATTTGGACTTTCCGCC
PDP156	ATTGTGAGCGGATAACAATTAAGCTTATGCTTTTATATAGGGAAAAGGTGGTGAACTACTATGGAAGAC GCCAAAAACATAAAG
PDP157	GCATGCGGCTAGCTGTCGACTAAGCTTTTACAATTTGGACTTTCCGCC
PDP160	AGTGTTGTTCCATTCCATTTCGGTTTTGGAATGTTTACT
PDP161	AGTAAACATTCCAAAACCGAAATGGAATGGAACAACACT
PDP174	TCTTTATGTTTTTGGCGTCTTCTTCTTCCTCTCTCATTGTTTC
PDP175	TCTTTATGTTTTTGGCGTCTTCTGCGAATTGTTTCATATTC

Table S3 Comparison of methods used to measure ATP concentrations

Effect of FCCP addition at 3.5 h poststarvation				
Method	Compartment	FCCP[a]	[ATP][b]	-/+ FCCP ratio
Luc H245F	MC	-	0.031 ± 0.004	5.2
		+	0.006 ± 0.001	
	FS	-	0.025 ± 0.005	6.3
		+	0.004 ± 0.002	
	total	-	0.056	5.6
		+	0.010	
extraction	total	-	0.48 ± 0.03	5.3
		+	0.09 ± 0.03	
Luc H245 total/extraction total		-	0.12	
		+	0.11	

Effect of IPTG addition to growing cells			
Method	IPTG[c]	[ATP][d]	-/+ IPTG ratio
Luc H245F	-	0.005 ± 0.003	0.6
	+	0.008 ± 0.002	
extraction	-	6 ± 2	1
	+	6 ± 4	
Luc H245F/extraction	-	0.0008	
	+	0.001	

Measurements at 6 h versus 3.5 h poststarvation				
Method	Compartment	Poststarvation time (h)	[ATP][e]	6/3.5 h ratio
Luc H245F	MC	6	0.054 ± 0.004	1.7
		3.5	0.031 ± 0.003	
	FS	6	0.034 ± 0.014	1.4
		3.5	0.025 ± 0.004	
	total	6	0.088	1.6
		3.5	0.056	
extraction	total	6	0.24 ± 0.02	0.6
		3.5	0.40 ± 0.06	
Luc H245F total/extraction total		6	0.37	
		3.5	0.14	

[a]FCCP (100 μM) was added (+) or withheld (-) for 15 min before measuring the ATP concentration at 3.75 h PS.

[b]The relative ATP concentration in arbitrary units (AU) was calculated from the data shown in Figure 2C and 2D for the Luc H245F method. For the extraction method, the ATP concentration (μM) is from Figure S1.

[c]IPTG (100 μM) was added (+) or withheld (-) for 30 min before measuring the ATP concentration.

[d]The relative ATP concentration (AU) is from Figure S4F for the Luc H245F method and the ATP concentration (μM) is from Figure S4C for the extraction method.

[e]The relative ATP concentration (AU) is from Figure 3D for the Luc H245F method and the ATP concentration (μM) is from Figure S6 for the extraction method.

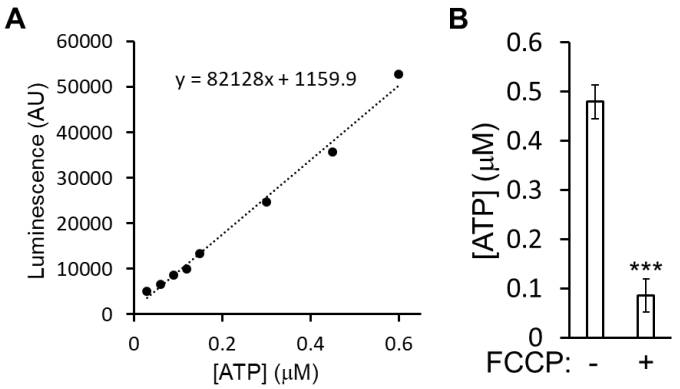

Fig. S1. FCCP treatment during sporulation lowers the ATP concentration in cell extracts. **(A)** ATP assay calibration. ATP solutions of known concentration were mixed with luciferin and firefly lantern extract containing Luc, and luminescence intensity was measured. The luminescence in arbitrary units (AU) is plotted versus the ATP concentration. The dashed line is the trend line of the data and the equation of the trend line is shown. **(B)** ATP concentration of extracts of cells treated with FCCP or left untreated. *B. subtilis* engineered to produce Luc H245F in the MC was starved to induce sporulation. At 3.5 h PS, the culture was split and subcultures were left untreated as a control (-) or were treated with 100 μM FCCP (+) for 15 min. ATP assays were performed on cell extracts in parallel with those shown in panel A. The ATP concentration of each extract was calculated using the trend line equation. The graph shows the average of three biological replicates and error bars represent one standard deviation. Three asterisks (***) indicates $P < 0.0005$ in a paired two-tailed *t*-test comparing the data for the untreated control with the FCCP-treated sample.

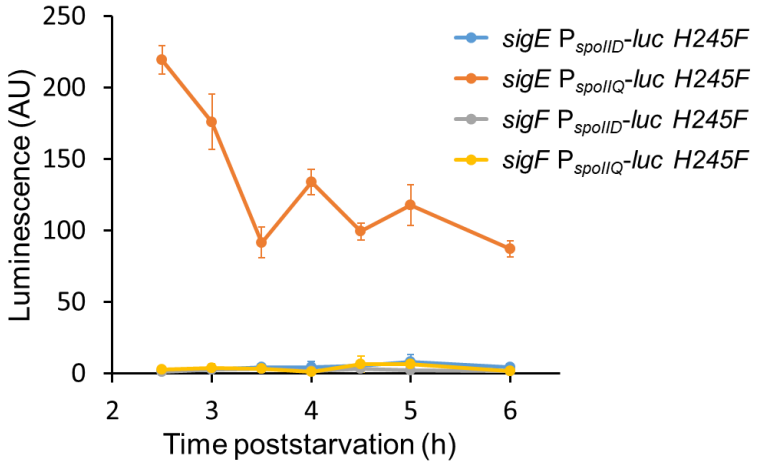

Fig. S2. Expression of *luc H245F* from the *spoIID* and *spoIIQ* promoters exhibits the expected pattern of dependence in *sigF* and *sigE* mutants. *B. subtilis* mutants unable to produce σ^E or σ^F due to a null mutation in *sigE* or *sigF*, respectively, were engineered to express *luc H245F* from the σ^E-dependent *spoIID* promoter or the σ^F-dependent *spoIIQ* promoter. The mutants were starved to induce sporulation. At 2 h PS, culture aliquots were transferred to a 96-well plate containing luciferin and the luminescence intensity was measured in arbitrary units (AU) at the indicated times PS. The graph shows the average of four or five biological replicates and error bars represent one standard deviation.

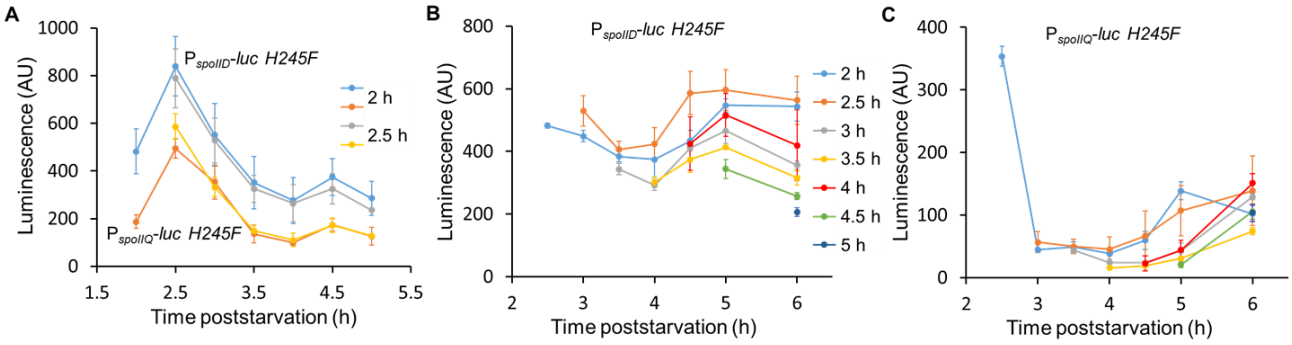

Fig. S3. Luminescence intensity following luciferin addition at different times during sporulation. *B. subtilis* strains engineered to produce Luc H245F in the MC from the *spoIID* promoter or in the FS from the *spoIIQ* promoter were starved to induce sporulation. At 2 h PS, culture aliquots were transferred to a 96-well plate. Luciferin was added at the time PS indicated in the legend and the luminescence intensity was measured in arbitrary units (AU) at the indicated times PS. **(A)** Luminescence intensity after luciferin addition at 2 or 2.5 h. The graph shows the average of three biological replicates each with four technical replicates and error bars represent one standard deviation for the strains with P_{spoIID}-*luc H245F* or P_{spoIIQ}-*luc H245F*. **(B)** MC luminescence intensity after luciferin addition at 2 h or later. The graph shows the average of three or four biological replicates (no technical replicates) and error bars represent one standard deviation for the strain with P_{spoIID}-*luc H245F*. **(C)** FS luminescence intensity after luciferin addition at 2 h or later. The experiment was the same as described for panel B, but using the strain with P_{spoIIQ}-*luc H245F*.

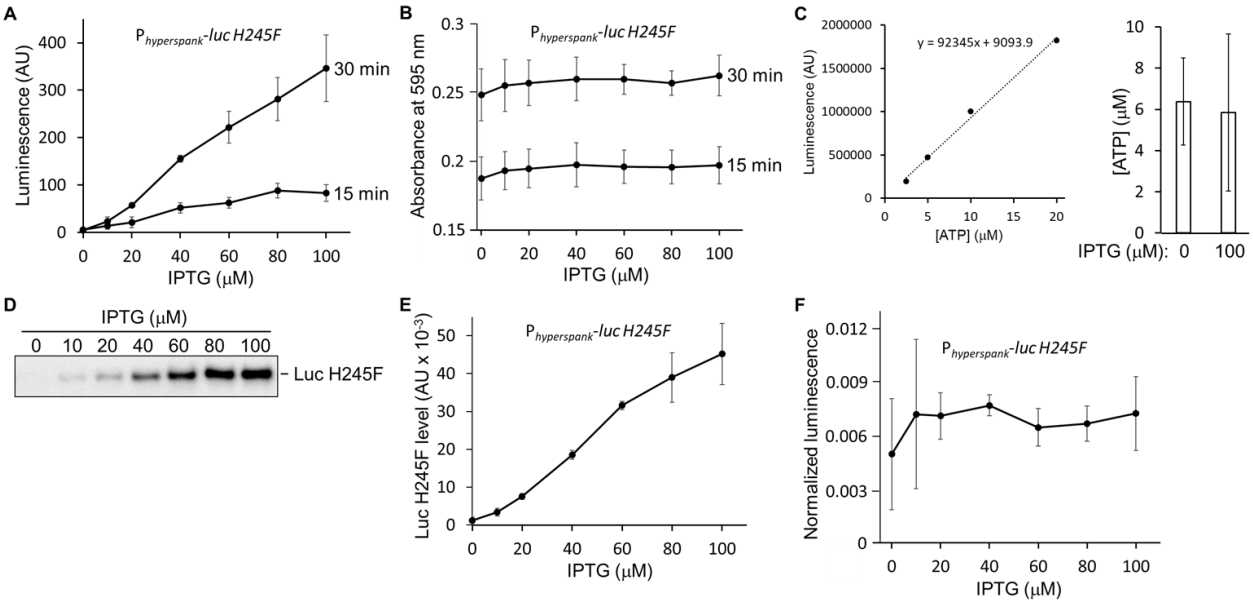

Fig. S4. Luc H245F, produced at different levels by expressing *luc H245F* from an IPTG-inducible promoter during growth, appears to be limiting for luminescence over a broad range since luminescence intensity normalized to the Luc H245F level is nearly constant. *B. subtilis* engineered to express *luc H245F* from the IPTG-inducible *hyperspank* promoter was grown until the culture reached the exponential phase of growth, then culture aliquots were transferred to a 96-well plate containing luciferin and IPTG (0-100 μM final concentrations as indicated). **(A)** Luminescence. The luminescence intensity was measured in arbitrary units (AU) after 15 and 30 min of additional growth. **(B)** Absorbance. The absorbance at 595 nm was measured at the same times as in panel A. **(C)** ATP concentration of extracts of cells treated with IPTG or left untreated for 30 min. The graph on the left shows the ATP assay calibration for this experiment (see the legend of Fig. S1 for explanation). Results are summarized in the graph on the right. IPTG addition did not significantly change the concentration of ATP in extracts ($P > 0.05$ in a paired two-tailed *t*-test). **(D)** Representative immunoblot showing Luc H245F levels in cells treated with IPTG or left untreated for 30 min. **(E)** Luc H245F levels in cells treated as in panel D. Each Luc H245F signal was quantified and normalized to a control sample (from the strain producing Luc H245F in the MC at 3.5 h PS) on the same blot. **(F)** Normalized luminescence of aliquots treated with IPTG or left untreated for 30 min. For each biological replicate, the luminescence intensity (measured as described for panel A) was divided by the Luc H245F level (measured as described for panel E) to yield a normalized value. The graphs show the average of at least three biological replicates and error bars represent one standard deviation, except the ATP assay calibration in panel C.

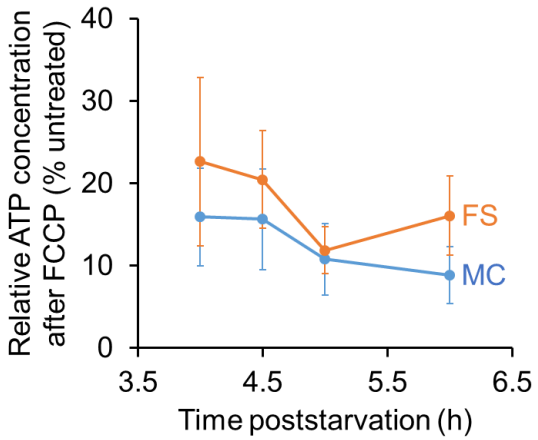

Fig. S5. Luc H245F detects decreases in the relative ATP concentration in both compartments after FCCP treatment during sporulation. *B. subtilis* strains engineered to synthesize Luc H245F in the MC or the FS were starved to induce sporulation. At 2 h PS, culture aliquots were transferred to a 96-well plate. At 15 min before the indicated times PS, aliquots were treated with FCCP (100 μM) or left untreated as controls, prior to measuring the luminescence intensity and the Luc H245F level by immunoblot analysis with anti-Luc antibodies at the indicated times. For each biological replicate, the luminescence was divided by the Luc H245F level to yield a normalized value. The normalized value after FCCP treatment was divided by the normalized value of the untreated control to yield the relative ATP concentration after FCCP treatment as a percentage of the untreated control. The graph shows the average of three biological replicates and error bars represent one standard deviation. The relative ATP concentration after FCCP treatment did not differ significantly comparing the data for the MC with the FS at the same time PS ($P > 0.05$ in Student's two-tailed *t*-tests).

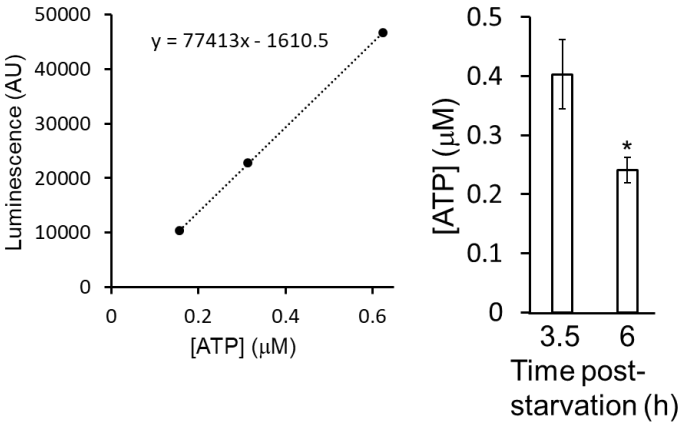

Fig. S6. ATP concentration of extracts of cells at different times during sporulation. *B. subtilis* engineered to produce Luc H245F in the MC was starved to induce sporulation. At 2 h PS, culture aliquots were transferred to a 96-well plate. Samples were collected at 3.5 and 6 h PS for preparation of cell extracts and ATP assays. The graph on the left shows the ATP assay calibration for this experiment (see the legend of Fig. S1 for explanation). ATP assays were performed on cell extracts in parallel. The ATP concentration of each extract was calculated using the trend line equation. The graph on the right shows the average of three biological replicates and error bars represent one standard deviation. The asterisk (*) indicates $P < 0.05$ in a paired two-tailed *t*-test comparing the data for 3.5 h PS with 6 h PS.

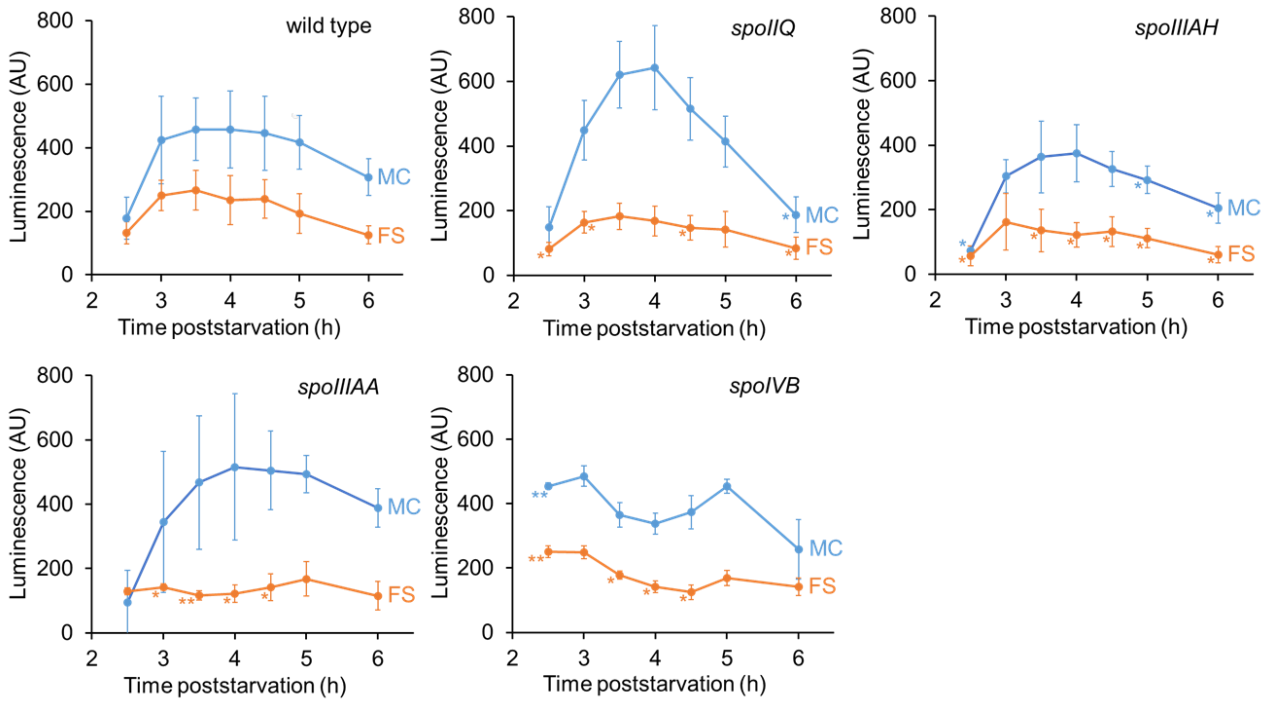

Fig. S7. Luminescence intensity from Luc H245F produced in the mother cell or the forespore during sporulation. *B. subtilis* strains engineered to synthesize Luc H245F in the MC or the FS were starved to induce sporulation. At 2 h PS, culture aliquots were transferred to a 96-well plate and the luminescence intensity was measured in arbitrary units (AU) at the indicated times PS. The wild-type strain (same data as Fig. 3B) is shown for comparison to the indicated mutants. Luminescence intensity is plotted on the same scale in each graph to facilitate comparison. Graphs show the average of three or four biological replicates and error bars represent one standard deviation. One asterisk (*) indicates $P < 0.05$ and two asterisks (**) indicate $P < 0.005$ in Student's two-tailed *t*-tests comparing the data for each mutant with WT cells at the same time PS.

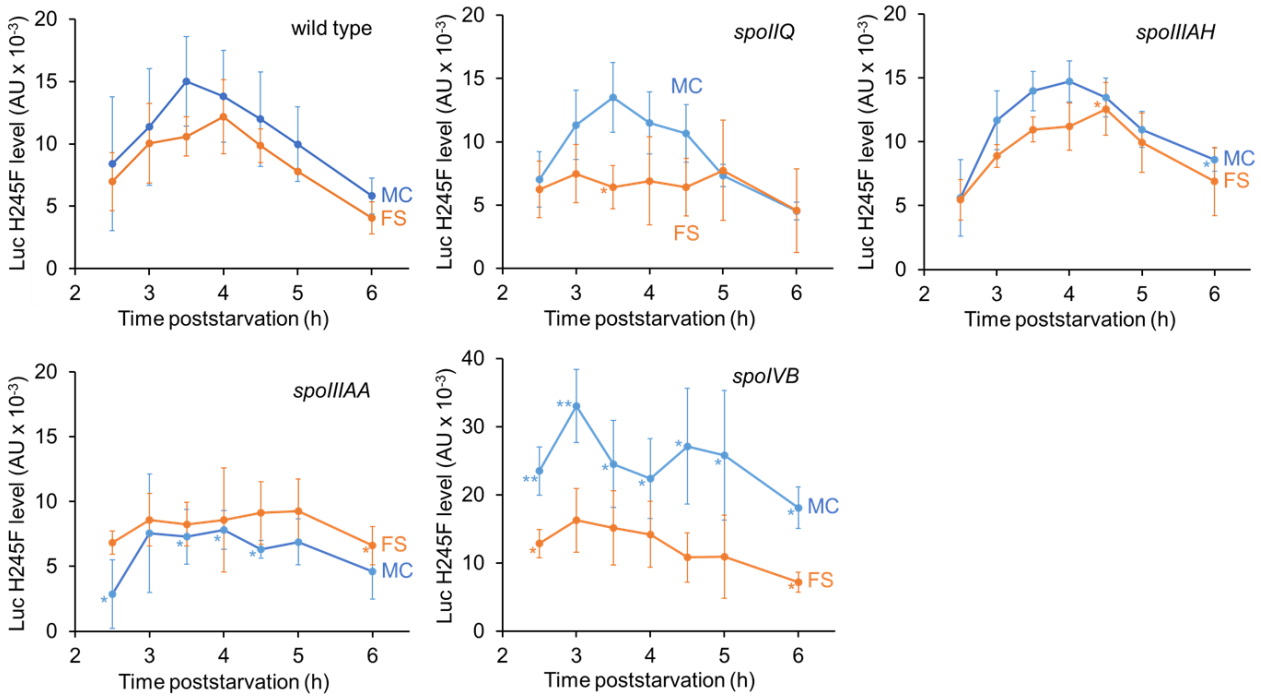

Fig. S8. Luc H245F levels in the mother cell and the forespore during sporulation. *B. subtilis* strains engineered to make Luc H245F in the MC or the FS were starved to induce sporulation. At 2 h PS, culture aliquots were transferred to a 96-well plate and the Luc H245F level was measured by immunoblot analysis with anti-Luc antibodies, in arbitrary units (AU) at the indicated times PS. Each Luc H245F signal was quantified and normalized to a control sample (from the strain synthesizing Luc H245F in the MC at 3.5 h PS) on the same blot. The wild-type strain (same data as Fig. 3C) is shown for comparison to the indicated mutants. The Luc H245F level is plotted on the same scale in each graph to facilitate comparison, except the *spoIVB* mutant. Graphs show the average of three or four biological replicates and error bars represent one standard deviation. One asterisk (*) indicates $P < 0.05$ and two asterisks (**) indicate $P < 0.005$ in Student's two-tailed *t*-tests comparing the data for each mutant with WT cells at the same time PS.

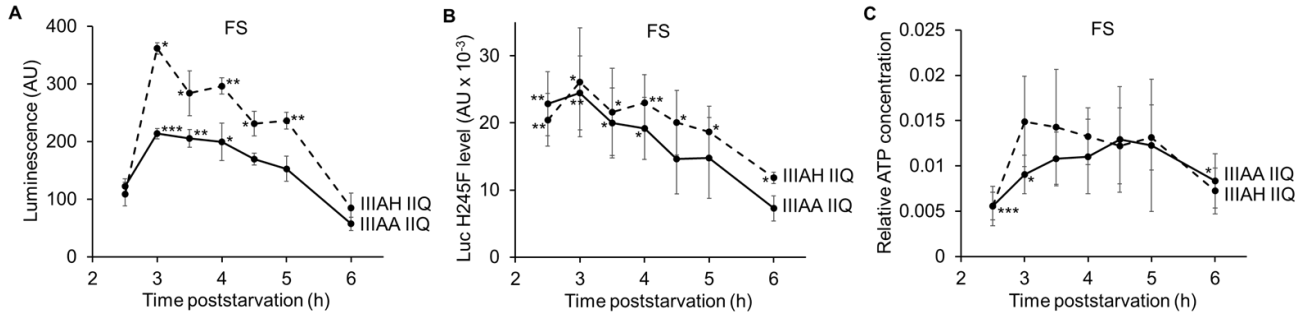

Fig. S9. The relative ATP concentration in the forespore remains low in *spoIIIAA/spoIIQ* and *spoIIIAH/spoIIQ* double mutants. *B. subtilis* mutants unable to produce the indicated channel proteins and engineered to make Luc H245F in the FS were starved to induce sporulation. At 2 h PS, culture aliquots were transferred to a 96-well plate, and at the indicated times PS the luminescence intensity was measured in arbitrary units (AU) and the Luc H245F level assessed by immunoblot analysis with anti-Luc antibodies. **(A)** Luminescence intensity. **(B)** Luc H245F level. Each Luc H245F signal was quantified and normalized to a control sample (from the strain producing Luc H245F in the MC at 3.5 h PS) on the same blot. **(C)** Relative ATP concentration. For each biological replicate, the luminescence intensity was divided by the Luc H245F level to yield a normalized value representing the relative ATP concentration. Graphs show the average of three biological replicates and error bars represent one standard deviation. One asterisk (*) indicates $P < 0.05$, two asterisks (**) indicate $P < 0.005$, and three asterisks (***) indicate $P < 0.0005$ in Student's two-tailed *t*-tests comparing the data for the *spoIIIAA/spoIIQ* and *spoIIIAH/spoIIQ* double mutants with the *spoIIIAA* and *spoIIIAH* single mutants, respectively, at the same time PS.

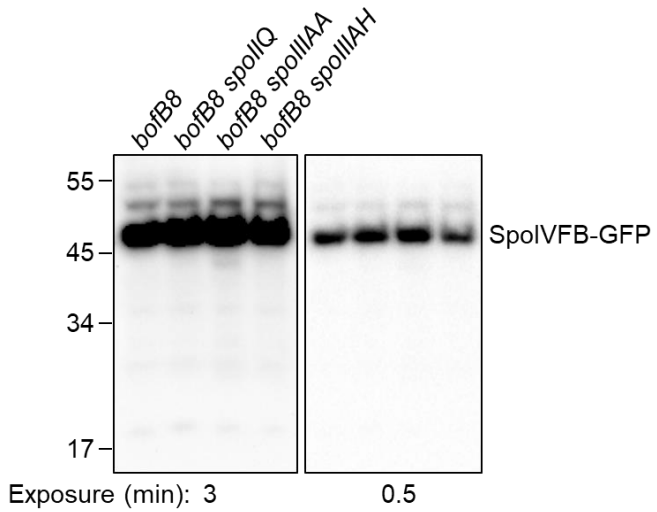

Fig. S10. SpoIVFB-GFP accumulates similarly in bypass mutants. *B. subtilis* strains with the *bofB8* mutation alone or in combination with a null mutation in *spoIIQ*, *spoIIIAA*, or *spoIIIAH*, and with *gfp* fused to *spoIVFB*, were starved to induce sporulation. All these strains have a null mutation in *sigG*, which is bypassed by the *bofB8* mutation (Cutting *et al.*, 1990). Samples collected at 3 h PS were subjected to immunoblot analysis using antibodies against GFP. The left panel shows a 3 min exposure to demonstrate that very little or no free GFP (27 kDa) accumulated. The molecular weight (kDa) and migration position of marker proteins are indicated. The right panel shows a 0.5 min exposure of the same blot to demonstrate that the SpoIVFB-GFP level was similar in all the strains.

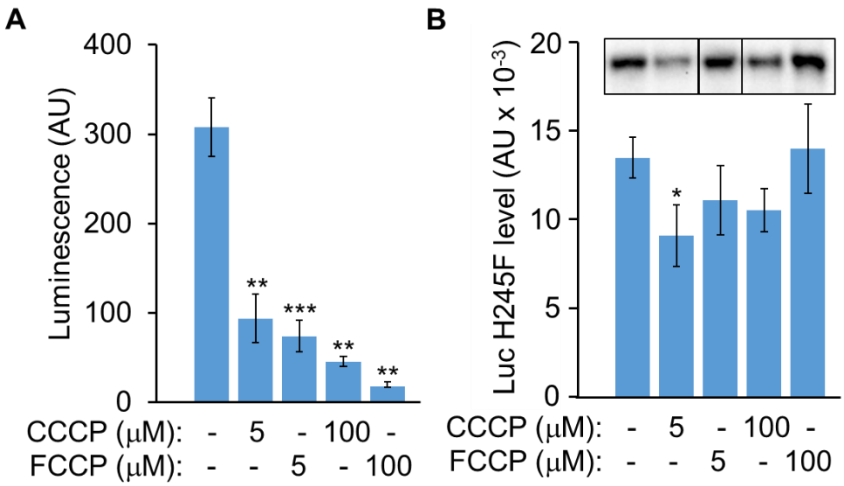

Fig. S11. Mother cell luminescence intensities and Luc H245F levels after treatment with ionophores during sporulation. *B. subtilis* engineered to produce Luc H245F in the MC was starved to induce sporulation. At 3.5 h PS, culture aliquots were transferred to a 96-well plate containing luciferin. Aliquots were left untreated as controls (-) or were treated with an ionophore as indicated for 15 min, prior to measuring **(A)** the luminescence intensities in arbitrary units (AU) and **(B)** the Luc H245F levels in AU by immunoblot analysis with anti-Luc antibodies. In panel B, each Luc H245F signal was quantified and normalized to a control sample (from the strain synthesizing Luc H245F in the MC at 3.5 h PS) on the same blot. A representative immunoblot is shown at the top (vertical lines indicate intervening lanes were removed). Graphs show the average of three biological replicates and error bars represent one standard deviation. One asterisk (*) indicates $P < 0.05$, two asterisks (**) indicate $P < 0.005$, and three asterisks (***) indicate $P < 0.0005$ in paired two-tailed *t*-tests comparing the data for the untreated control with the treated sample.

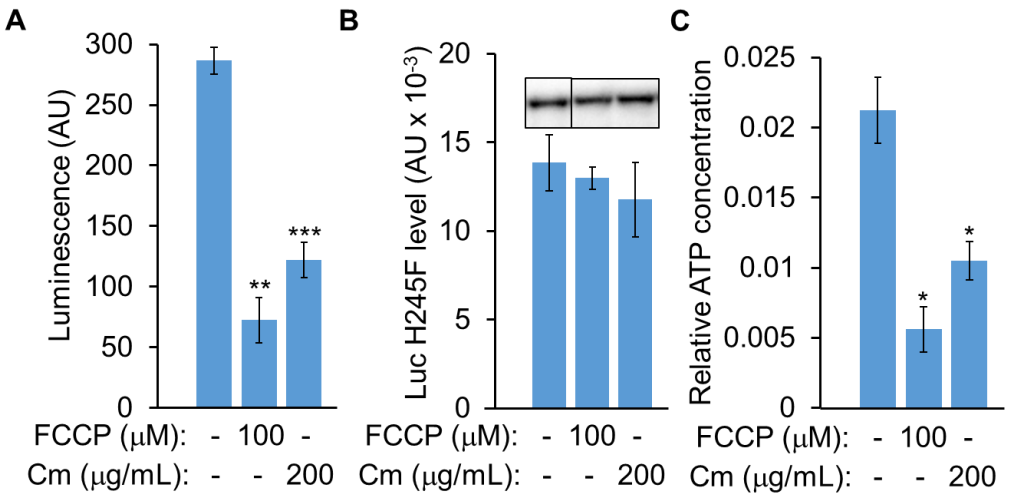

Fig. S12. Chloramphenicol decreases the mother cell ATP concentration. *B. subtilis* engineered to make Luc H245F in the MC was starved to induce sporulation. At 3.5 h PS, culture aliquots were transferred to a 96-well plate containing luciferin. Aliquots were left untreated as controls (-) or were treated with FCCP or Cm as indicated for 15 min, prior to measuring **(A)** the luminescence intensities in arbitrary units (AU) and **(B)** the Luc H245F levels in AU by immunoblot analysis with anti-Luc antibodies. In panel B, each Luc H245F signal was quantified and normalized to a control sample (from the strain producing Luc H245F in the MC at 3.5 h PS) on the same blot. A representative immunoblot is shown at the top (vertical lines indicate intervening lanes were removed). **(C)** Relative ATP concentration. The luminescence intensity was divided by the Luc H245F level to yield a normalized value representing the relative ATP concentration. Graphs show the average of three biological replicates and error bars represent one standard deviation. One asterisk (*) indicates $P < 0.05$, two asterisks (**) indicate $P < 0.005$, and three asterisks (***) indicate $P < 0.0005$ in paired two-tailed *t*-tests comparing the data for the untreated control with the treated sample.

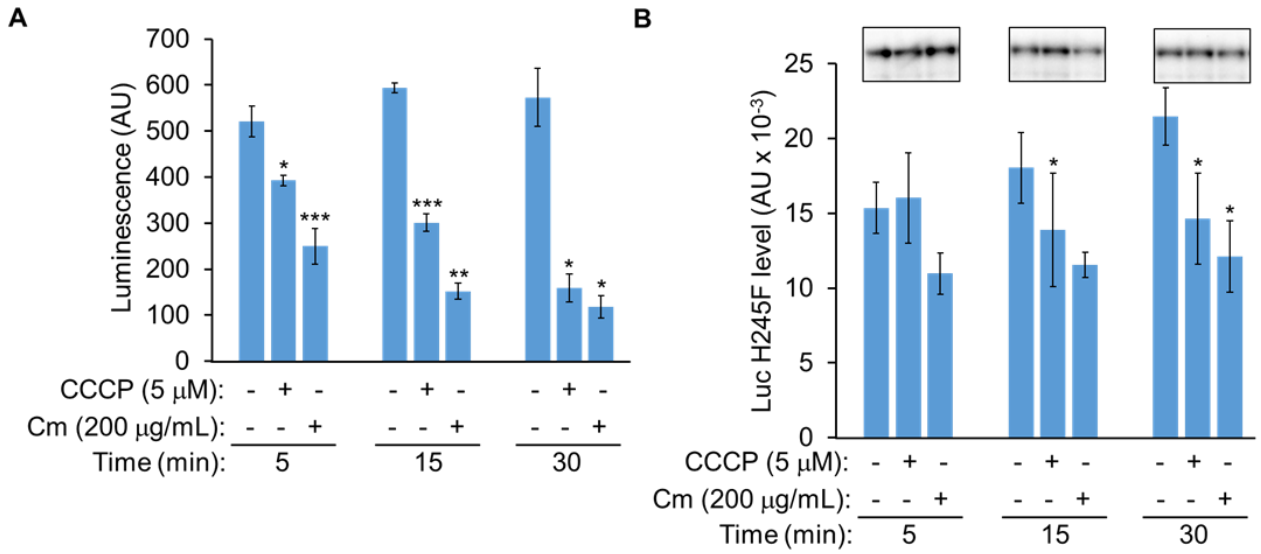

Fig. S13. Mother cell luminescence intensities and Luc H245F levels after CCCP or Cm treatment. *B. subtilis* engineered to produce Luc H245F in the MC was starved to induce sporulation. At 2.25 h PS, culture aliquots were transferred to a 96-well plate containing luciferin. At 2.5 h, aliquots were left untreated as controls (-) or were treated with FCCP or Cm as indicated, prior to measuring **(A)** the luminescence intensities in arbitrary units (AU) and **(B)** the Luc H245F levels in AU by immunoblot analysis with anti-Luc antibodies, at 5, 15, and 30 min after treatment. In panel B, each Luc H245F signal was quantified and normalized to a control sample (from the strain synthesizing Luc H245F in the MC at 3.5 h PS) on the same blot. A representative immunoblot is shown at the top (vertical lines indicate intervening lanes were removed). Graphs show the average of three biological replicates and error bars represent one standard deviation. One asterisk (*) indicates $P < 0.05$, two asterisks (**) indicate $P < 0.005$, and three asterisks (***) indicate $P < 0.0005$ in paired two-tailed *t*-tests comparing the data for the untreated control with the treated sample.

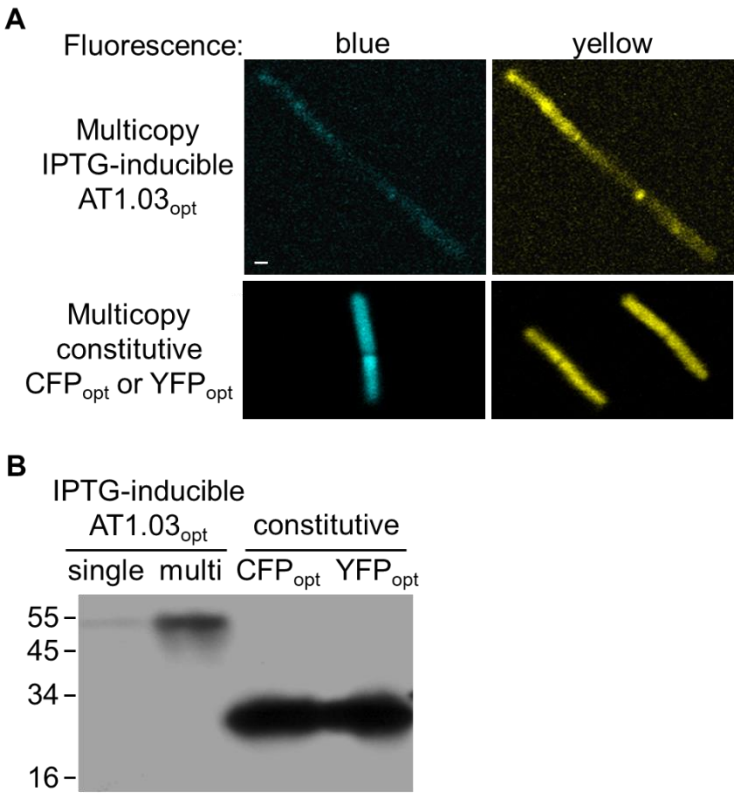

Fig. S14. Analysis of *B. subtilis* designed to produce a FRET-based ATP sensor. (A) Fluorescence microscopy. The top panels show a single filamentous cell after induction with IPTG for 2 h to express the gene encoding AT1.03$_{opt}$ from a multicopy plasmid. The bottom panels show dividing cells constitutively expressing the genes for CFP$_{opt}$ (left) or YFP$_{opt}$ (right) from a multicopy plasmid. The photomultiplier tube high voltage setting was adjusted to be more sensitive in order to visualize the cells shown in the top panels, which explains the higher background fluorescence than in the bottom panels. All panels are at the same scale and in the top-left panel the scale bar = 1 μm. **(B)** Immunoblot analysis. *B. subtilis* designed to express the gene for AT1.03$_{opt}$ from a single copy at the chromosomal *amyE* locus or from a multicopy plasmid were induced with IPTG for 2 h. For comparison, *B. subtilis* designed to constitutively express genes for CFP$_{opt}$ or YFP$_{opt}$ from a multicopy plasmid were grown to the mid-log phase. Samples were subjected to immunoblot analysis using antibodies against GFP. The molecular weight (kDa) and migration of marker proteins is indicated.

References

Ando, T., Imamura, H., Suzuki, R., Aizaki, H., Watanabe, T., Wakita, T., and Suzuki, T. (2012) Visualization and measurement of ATP levels in living cells replicating hepatitis C virus genome RNA. *PLoS Pathog.* **8**: e1002561.

Cutting, S., Driks, A., Schmidt, R., Kunkel, B., and Losick, R. (1991) Forespore-specific transcription of a gene in the signal transduction pathway that governs pro-σ^K processing in *Bacillus subtilis*. *Genes Dev.* **5**: 456-466.

Cutting, S., Oke, V., Driks, A., Losick, R., Lu, S., and Kroos, L. (1990) A forespore checkpoint for mother-cell gene expression during development in *Bacillus subtilis*. *Cell* **62**: 239-250.

Cutting, S.M., and Horn, P.B.V., (1990) Genetic analysis. In: Molecular Biological Methods for *Bacillus.* C.R. Harwood & S.M. Cutting (eds). New York: John Wiley & Sons, pp. 27-74.

Doan, T., Morlot, C., Meisner, J., Serrano, M., Henriques, A.O., Moran, C.P., Jr., and Rudner, D.Z. (2009) Novel secretion apparatus maintains spore integrity and developmental gene expression in *Bacillus subtilis*. *PLoS Genet.* **5**: e1000566.

Fortnagel, P., and Freese, E. (1968) Analysis of sporulation mutants. II. Mutants blocked in the citric acid cycle. *J. Bacteriol.* **95**: 1431-1438.

Freese, E., and Fortnagel, U. (1969) Growth and sporulation of *Bacillus subtilis* mutants blocked in the pyruvate dehydrogenase complex. *J. Bacteriol.* **99**: 745-756.

Gibson, D.G., Young, L., Chuang, R.Y., Venter, J.C., Hutchison, C.A., 3rd, and Smith, H.O. (2009) Enzymatic assembly of DNA molecules up to several hundred kilobases. *Nat. Methods* **6**: 343-345.

Hutchison, K.W., and Hanson, R.S. (1974) Adenine nucleotide changes associated with the initiation of sporulation in *Bacillus subtilis*. *J. Bacteriol.* **119**: 70-75.

Imamura, H., Nhat, K.P., Togawa, H., Saito, K., Iino, R., Kato-Yamada, Y., Nagai, T., and Noji, H. (2009) Visualization of ATP levels inside single living cells with fluorescence resonance energy transfer-based genetically encoded indicators. *Proc. Natl. Acad. Sci. USA* **106**: 15651-15656.

Klofat, W., Piaciolo, G., Chappella, E.W., and Freese, E. (1969) Production of adenosine triphosphate in normal cells and sporulation mutants of *Baciilus subtilis*. *J. Biol. Chem.* **244**: 3270-3276.

Mirouze, N., Prepiak, P., and Dubnau, D. (2011) Fluctuations in *spo0A* transcription control rare developmental transitions in *Bacillus subtilis*. *PLoS Genet.* **7**: e1002048.

Rudner, D.Z., and Losick, R. (2002) A sporulation membrane protein tethers the pro-σ^K processing enzyme to its inhibitor and dictates its subcellular localization. *Genes Dev.* **16**: 1007-1018.

Sambrook, J., Fritsch, E.F., and Maniatis, T., (1989) *Molecular cloning: a laboratory manual, 2nd ed.* Cold Spring Harbor Laboratory Press, Cold Spring Habor, NY.

Sandman, K., Kroos, L., Cutting, S., Youngman, P., and Losick, R. (1988) Identification of the promoter for a spore coat protein gene in *Bacillus subtilis* and studies on the regulation of its induction at a late stage of sporulation. *J. Mol. Biol.* **200**: 461-473.

Sastalla, I., Chim, K., Cheung, G.Y., Pomerantsev, A.P., and Leppla, S.H. (2009) Codon-optimized fluorescent proteins designed for expression in low-GC gram-positive bacteria. *Appl. Environ. Microbiol.* **75**: 2099-2110.

Schneider, D.A., and Gourse, R.L. (2004) Relationship between growth rate and ATP concentration in *Escherichia coli*: a bioassay for available cellular ATP. *J. Biol. Chem.* **279**: 8262-8268.

Segev, E., Smith, Y., and Ben-Yehuda, S. (2012) RNA dynamics in aging bacterial spores. *Cell* **148**: 139-149.

Setlow, P., and Kornberg, A. (1970) Biochemical studies of bacterial sporulation and germination. XXII. Energy metabolism in early stages of germination of *Bacillus megaterium* spores. *J. Biol. Chem.* **245**: 3637-3644.

Sharp, M.D., and Pogliano, K. (2002) Role of cell-specific SpoIIIE assembly in polarity of DNA transfer. *Science* **295**: 137-139.

Shimotsu, H., and Henner, D.J. (1986) Construction of a single-copy integration vector and its use in analysis of regulation of the *trp* operon of *Bacillus subtilis*. *Gene* **43**: 85-94.

Singh, R.P., Setlow, B., and Setlow, P. (1977) Levels of small molecules and enzymes in the mother cell compartment and the forespore of sporulating Bacillus megaterium. *J. Bacteriol.* **130**: 1130-1138.

Stragier, P., Bonamy, C., and Karmazyn-Campelli, C. (1988) Processing of a sporulation sigma factor in *Bacillus subtilis*: How morphological structure could control gene expression. *Cell* **52**: 697-704.

Strahl, H., and Hamoen, L.W. (2010) Membrane potential is important for bacterial cell division. *Proc. Natl. Acad. Sci. USA* **107**: 12281-12286.

Youngman, P., Perkins, J.B., and Losick, R. (1984) Construction of a cloning site near one end of Tn*917* into which foreign DNA may be inserted without affecting transposition in *Bacillus subtilis* or expression of the transposon-borne *erm* gene. *Plasmid* **12**: 1-9.

Yousten, A.A., and Hanson, R.S. (1972) Sporulation of tricarboxylic acid cycle mutants of *Bacillus subtilis*. *J. Bacteriol.* **109**: 886-894.

Zhou, R., and Kroos, L. (2004) BofA protein inhibits intramembrane proteolysis of pro-σ^K in an intercompartmental signaling pathway during *Bacillus subtilis* sporulation. *Proc. Natl. Acad. Sci. USA* **101**: 6385-6390.